






# Evaluation of Satellite and Reanalysis Models for Solar Irradiance Estimation in Northwest Argentina

Rubén Ledesma , Rodrigo Alonso-Suárez , Germán Salazar , Fernando Nollas , and Olga Vilela 

**Abstract**—Accurate solar resource assessment is critical for the development of solar energy projects, especially in regions with complex climatic and geographic conditions. This study evaluates the performance of various satellite-based and reanalysis models in estimating global horizontal irradiance (GHI) in Northwestern Argentina, focusing on two locations characterized by different environmental conditions: La Quiaca and Salta. Five satellite-based models (CAMS Heliosat-4, NREL NSRDB, GOES DSR, LSA-SAF MDSSFTD, and GOES G-CIM) and two reanalysis datasets (MERRA-2 and ERA-5) were analysed and compared with high-quality ground-based measurements recorded between 2020 and 2023. The results show that the G-CIM and NSRDB models provide the most accurate irradiance estimates, effectively minimising errors even in challenging environments with extreme altitude or variable terrain reflectivity. At the 10-minute time scale in Salta, the G-CIM model yields a root mean squared deviation (RMSD) of 23.4% and a mean bias of 4.8%, whereas the NSRDB model records an RMSD of 26.6% and a mean bias of  $-4.2\%$ . In La Quiaca, both models achieve RMSD values below 20% and mean biases under 1%. At the 60-minute scale, in Salta, G-CIM and NSRDB exhibit RMSDs of 20.7% and 19.7%, with corresponding mean biases of 5.4% and  $-3.6\%$ , respectively, while in La Quiaca they maintain mean biases below 1% and RMSDs of 13.2% for G-CIM and 12.6% for NSRDB. Conversely, the MERRA-2 and ERA-5 reanalysis models showed higher uncertainties, particularly in areas with significant microclimatic variations. The study highlights the importance of using locally validated satellite data for accurate solar resource assessment and emphasises the need for site-specific adjustments when applying global irradiance models. These findings contribute to improved planning and decision-making for solar energy projects in Northwest Argentina and provide valuable insights for researchers, policy makers and industry professionals.

Link to graphical and video abstracts, and to code:  
<https://latamtx.ieeet9.org/index.php/transactions/article/view/9498>

**Index Terms**—Global Horizontal Solar Irradiance, Satellite Models, Reanalysis Data, Solar Resource Assessment, Northwest Argentina.

## I. INTRODUCTION

The associate editor coordinating the review of this manuscript and approving it for publication was Bruno Henrique Groenner Barbosa (*Corresponding author: Rubén Darío Ledesma*).

Rubén Darío Ledesma, and G. Salazar are with the National University of Salta and the Institute for Research in Non-Conventional Energy, Salta, Argentina (e-mails: rldedesma@exa.unsa.edu.ar, and german.salazar@conicet.gov.ar).

R. Alonso-Suárez is with the Solar Energy Laboratory, CENUR Litoral Norte, University of the Republic, Uruguay (e-mail: rodrigoa@fing.edu.uy).

F. Nollas is with the Servicio Meteorológico Nacional Argentino, Argentina (e-mail: fnollas@smn.gob.ar).

O. Vilela is with the Center for Renewable Energy of the Federal University of Pernambuco, Brazil (e-mail: ocv@ufpe.br).

**I**N order to simulate and financially analyse solar energy projects, it is crucial to accurately assess the solar resource at the project location. Uncertainty in solar irradiance data is the primary factor influencing the economic risk assessment of large-scale photovoltaic (PV) solar power plants [1], [2]. Financial and engineering project analysis should ideally be based on at least a decade of site solar irradiance measurements, quality controlled according to an approved protocol. This type of long-term, quality-controlled measurement is usually not available, as it is unlikely that such consistent measurements have been taken in the vicinity of any given project site. In this context, close enough means less than 15–20 km from the project location, the breakthrough distance at which simple satellite estimates provide better accuracy than extrapolation or interpolation of ground measurements [3], [4].

To overcome this problem, modelled data from different sources can be used, such as satellite-based models (satellite solar data) or numerical atmospheric models (reanalysis solar data). These modelled data are typically available elsewhere, some freely available and some commercially available, with varying spatial and temporal resolution. Although they appear to solve the problem, modelled data can suffer from significant uncertainties that can affect the medium-term viability of solar energy projects [5], [6] due to inaccurate estimates of the return on investment. Therefore, these models need to be validated against ground-based data before use to diagnose biases and inaccuracies and to decide which source of information is most appropriate for a given region. The validity or relevance of a modelled dataset within a climatically affine area is then determined by comparing the simultaneous estimated values with those measured at a site within the area [7]–[11].

Satellite models are based on moderate-resolution, high-frequency geostationary imagery. They provide information on cloud cover over large areas with an intra-hourly update frequency of 10 or 15 minutes and a spatial resolution of 500–1000 metres per pixel. Since large solar power plants can cover more than one satellite pixel (e.g. for nominal power higher than 10 MW), satellite models are suitable for estimating the solar irradiance at the PV panels and thereby the output power [6]. It is worth noting that satellite models have the advantage of using actual cloud data rather than simulated cloud data, such as that from numerical atmospheric models, making them the most effective tool for assessing solar resources through remote sensing [9], [12]–[14]. Therefore, the use of satellite databases is recommended over reanalysis data for solar resource assessment, a claim that needs to be locally validated with good quality ground-based measurements, especially in complex terrains.

Northwest Argentina is a region of great interest for studying solar resources using satellite databases, for several reasons. One of them is the rich resource availability of the region, which exceeds the world average in its western part. In addition, the geographical variability and altitude differences generate microclimates that can be very different over short distances, from tens to hundreds of kilometres, significantly affecting the behaviour, distribution and average values of solar radiation. This also leads to very different ground albedo conditions, which are known to affect solar satellite data [15]–[17]. Finally, there is a lack of operational radiometric station networks with traceable sensors, quality control and proper maintenance. Although studies have reported on the performance of some satellite models for estimating solar irradiance in the Northwest region of Argentina [18]–[20], there is still no analysis that compares the estimates of several different models in a standardised framework. That is, a uniform evaluation of the different sources against measured data using the same quality procedures over the same period and sites.

This work then aims to fill this gap for Northwest Argentina by providing a thoughtful benchmark of several freely available modelled solar databases over different time scales. Two sites representing different conditions in the region are analysed: La Quiaca (LQ, 3,450 m above sea level) and Salta City (SA, 1,200 m above sea level). Due to their geographical characteristics, these sites have very different climates and cloudiness behaviour. For example, while clear sky days are the most common situation in LQ, different types of cloudy days can be observed in SA. Both sites are challenging for remote estimation of solar irradiance, but for different reasons. The SA site is close to a variable albedo terrain, which can confuse satellite models, especially depending on the pixel size. The LQ site has an extreme altitude and a very high ground albedo, which satellite models often misinterpret unless given special treatment. Taken together, both sites represent common situations and climates in the region. The main contribution of this article is therefore to establish a model ranking in the region, and to assess their typical accuracy under a unified framework at these representative sites. This sheds light on which modelled database is most suitable for solar radiation estimation in the area, a much-needed information for research studies, policy makers and solar industry practitioners. In addition, this article also presents a novel locally implemented model using the Cloud Index Model (CIM) framework, one of the most widely used modelling strategies for producing accurate and simple solar satellite models.

The remainder of this article is organized as follows. Section II describes the sites, the measured data and the quality control procedures used. Section III presents the satellite and reanalysis data sets used for comparison. Section IV gives a brief introduction to the evaluation metrics, and Section V presents the results and discussion. Finally, Section VI summarises our conclusions.

## II. GROUND MEASUREMENTS

The sites are detailed in Table I, including their identification code, location (deg), elevation (in meters above sea

level), and their corresponding classification in the updated Köppen-Geiger climate map [21]. Both sites are located close to the Southern Tropic (latitude  $-23.44$ ), one to the north and the other to the south. The SA station is located on the experimental campus of INENCO at the National University of Salta and is maintained periodically. It is a pre-Andean urban site with frequent cloud formation due to its location in a valley close to the Andes (Lerma Valley). The climate is a subtropical highland, temperate, with dry winters and cold summers (Cwb). The LQ station is part of the monitoring network of the Argentine National Meteorological Service. It is a semi-arid Andean cold steppe (BSk) with one of the highest sunshine hours values in Argentina. Both stations are equipped with class A or B pyranometers (according to ISO 9060:2018 standard) to measure global solar horizontal irradiance (GHI). An Eppley PSP pyranometer was used at the SA station and a Kipp & Zonen CMP11 pyranometer at the LQ station. Data were recorded at 1 minute intervals, with each value representing the average of six instantaneous samples taken every 10 seconds. This study analyses data collected over two years for each station: from 2020 to 2021 for LQ and from 2022 to 2023 for SA.

TABLE I  
GROUND MEASUREMENT STATIONS

CODE	Site	Latitude	Longitude	Altitude (m)	Climate
SA	Salta	-24.72	-65.42	1233	Cwb
LQ	La Quiaca	-22.10	-65.60	3468	BSk

The one-minute GHI measurements were subjected to the quality control procedure defined in Ref. [22]. The full procedure requires diffuse horizontal irradiance, but since this study only works with the GHI, a shorter version was used. Table II describes the filters used, where  $E$  is the solar constant,  $S$  is the Earth-Sun distance correction factor,  $\theta_z$  is the solar zenith angle, and  $kt$  is the dimensionless clearness index, defined as the ratio of the GHI to the horizontal irradiance at the top of the atmosphere.

TABLE II  
QUALITY CONTROL FILTERS APPLIED TO THE  
MEASUREMENTS

Filter	Description
F1	$GHI < 1.5 E S (\cos(\theta_z))^{1.2} + 100 \text{ W/m}^2$
F2	$GHI > (6.5331 - 0.065502 \theta_z + 1.8312E-4 \theta_z^2) / (1 + 0.01113 \theta_z)$
F3	$kt < 1.4 \ \& \ (90 - \theta_z) < 10^\circ$

The results of the quality control process applied to the SA and LQ stations demonstrate a significant reduction in the number of records after applying the filters. For the SA stations, out of a total of 329952 records, 253284 passed the Altitude Filter, representing approximately 77% of the initial dataset. For the LQ stations, out of a total of 524592 records, 362328 passed the Altitude Filter, which corresponds to 69% of the original dataset. These results highlight the effectiveness of the filter in refining the dataset, ensuring that only the most reliable records remain for subsequent analysis.

The measurement series were analyzed using the Standard Normal Homogeneity Test (SNHT) [23] to determine if the series displayed any changes in its behaviour resulting from an alteration or deviation in its normal trend. No alterations were detected in the series with  $p$ -values of 0.8 and 0.9.

### III. MODELS

Five satellite-based and two reanalysis-based estimation models for GHI are assessed. These models are described in this section. The GHI estimates can be freely downloaded from respective online portals. A local implementation of cloud index satellite model [24], [25] is also included.

#### A. CAMS Heliosat-4

Heliosat-4 [26] is a fully physical model that employs a rapid yet precise approach to the libRadtran radiative transfer model [27]. This model utilizes various satellite data and the reanalysis database from the Copernicus Atmosphere Monitoring Service (CAMS). Cloud properties are derived from Meteosat Second Generation (MSG) satellite images at a 15-minute time rate using an adapted APOLLO scheme (AVHRR3 Processing Scheme Over Clouds, Land, and Ocean) [28]. The operational version of Heliosat-4 takes the form of lookup tables, enabling rapid computation. This model has already been evaluated in the region in studies such as [18], [19]; however, these studies do not report comparisons with other modeled solar estimation data sets. This dataset was downloaded from the SoDa website with a time resolution of 15 minutes. The MSG pixel size over the region is about 16 km.

#### B. NREL NSRDB

The National Solar Radiation Database (NSRDB) uses the Physical Solar Model (PSM) [29]. This is a two-stage model that integrates cloud properties from GOES satellites ( $4 \times 4$  km, 30-minute intervals), aerosol optical depth from MODIS and MERRA-2 ( $0.5^\circ$  resolution, interpolated to  $4 \times 4$  km), and surface albedo from MODIS MCD43GF product (30 arc-seconds, 8-day intervals).

The PSM uses two radiative transfer models: REST2 for clear sky conditions and FARMS (Fast All-sky Radiation Model for Solar applications) [30] for all-sky conditions. FARMS uses precalculated cloud transmittances and reflectances parameterized as functions of solar zenith angle, cloud phase, optical thickness, and particle size. This approach makes FARMS about 1000 times faster than traditional two-stream methods while maintaining comparable accuracy. Data processing includes re-gridding inputs to  $4 \times 4$  km resolution and gap filling for missing cloud properties. For this work, the PSM v3.2.2 data was retrieved from the NSRDB website at a 10-minute time resolution.

#### C. GOES DSR

The GOES Downward Shortwave Radiation (DSR) product, developed by NESDIS/NOAA, uses the Enterprise Processing System (EPS) Shortwave Radiation Budget (SRB) hybrid

algorithm to estimate incident solar radiation reaching the Earth's surface and reflected solar radiation exiting the top of the atmosphere from visible and near-infrared GOES satellite imagery. This process involves several steps, including sensor data calibration, atmospheric correction for clear sky cases, and determination of the amount of clouds and aerosols present in the atmosphere [31].

The SRB algorithm is run at the pixel level, assigning each pixel to one of four categories: clear sky without snow/ice, clear sky with snow/ice, water cloud, and ice cloud. Two estimation paths are used: direct if the required Level 2 (L2) input data is available, and indirect otherwise. The direct path adapts the CERES [32], [33] model using precomputed lookup tables based on the Fu and Liou RTM, taking into account L2 satellite products such as surface albedo, aerosol optical depth, and aerosol single scattering albedo for clear sky scenes, and cloud optical depth, radius, and top height for cloudy scenes. The indirect path uses the climatological values of aerosol optical depth and single scattering albedo for the given date if the pixel is clear sky. If the pixel is cloudy, the atmospheric transmission is estimated using the top of the atmosphere albedo derived from the imager reflectances. This model in the region of interest has a spatial resolution of  $0.5 \times 0.5^\circ$  in latitude and longitude, and a temporal update frequency of 60 minutes.

It is important to note that this model exhibits a significant number of gaps in its estimates, particularly for values with a solar zenith angle (SZA) greater than  $70^\circ$ . To facilitate the comparative analysis, these estimates were interpolated using a method similar to that proposed in Ref. [34]. The GHI values modeled by DSR were linearly interpolated based on the DSR-modeled clearness index.

#### D. LSA-SAF MDSSFTD

The MSG Downwelling Surface Short-wave Radiation Fluxes - Total and Diffuse (MDSSFTD) product is an instantaneous (every 15 minutes) estimate of the global and diffuse downward shortwave radiation flux at the surface. The method for retrieving this product consists of two separate modules: one for clear sky and one for cloudy sky conditions [35], [36]. The clear sky product uses the approach described in Ref. [37]. This method, known as SIRAMix (Surface Incident Radiation using Aerosol Mixtures), is a physical parameterization method coupled to a pre-calculated lookup table (LUT) of aerosol properties, consisting mainly of the direct and diffuse transmittances of the different aerosol components and their corresponding aerosol albedos. The LUT is generated using radiative transfer models to vary aerosol loading, water vapor, and solar zenith angle. The cloudy GHI retrieval method uses the total shortwave cloud albedo at the top of the atmosphere (TOA) obtained from the observed TOA reflectances of the MSG. It uses the same aerosol estimates as in the clear sky case, and cloud-related terms are determined using a simplified radiative transfer model, similar to the method in Ref. [38]. Finally, these transmittances, namely the effective clear-sky transmittance estimated using gases and aerosols and the cloud transmittance estimated using the simplified radiative transfer model, are used together to determine the GHI.

This model has an approximate spatial resolution of 3 km with a 15-minute update frequency, and its estimates can be downloaded in NetCDF format from <https://datasasaf.lasvcs.ipma.pt/PRODUCTS/MSG/MDSSFTD/>.

#### E. GOES G-CIM

The final satellite-based model tested in this work is a locally implemented model. It is a Cloud Index Model (CIM) implemented using visible channel images from the GOES-16 satellite, similar to Refs. [24] and [25]. The model formulation is:

$$\text{GHI} = \text{GHI}_{\text{csk}} \times F(\eta) \text{ with } \eta = \frac{\rho - \rho_{\min}}{\rho_{\max} - \rho_{\min}}, \quad (1)$$

where  $\rho$  is the Earth reflectance value obtained for each site from the GOES-16 visible channel images,  $\text{GHI}_{\text{csk}}$  are clear sky estimates from the Argpv2 model [39],  $F$  is a cloud attenuation factor, and  $\eta$  is the cloud index [40]. The value of  $\rho_{\max}$  was set to 80% as in Refs. [25], [41], and  $\rho_{\min}$  was calculated as the average of the twenty minimum values of  $\rho$  in a 300-hour moving window centered on the point of interest as proposed in Ref. [18]. The cloud attenuation function is defined as  $F(\eta) = (a * \eta + b)$ . The Argpv2 clear sky model has a local adjustment for the study region of this work. The values of  $a$  and  $b$  were locally calibrated for each site using 50% of the data in a shuffled cross-validation process. The resulting parameters were  $a = -0.804$  and  $b = 0.998$  for SA, and  $a = -0.807$  and  $b = 1.000$  for LQ.

#### F. MERRA-2

The *Modern-Era Retrospective Analysis for Research and Applications, version 2* (MERRA-2) [42] is a reanalysis dataset developed by NASA with the Goddard Earth Observing System (GEOS-5.12.4) atmospheric data assimilation system [43], [44]. It is used to estimate various atmospheric parameters, including the downward shortwave irradiance, the GHI. The dataset covers the period from 1980 to the present with a latitude-longitude spatial resolution of  $0.5 \times 0.625^\circ$  and a time step of 60 minutes. This model improves the modeling of aerosols and related information affecting clear sky solar irradiance from the previous MERRA version 1 [45]. It also includes other physical improvements, such as water vapor content and cloud modeling [46], that affect solar irradiance estimates under all sky conditions. As a result of these updates, the dataset is expected to provide better solar irradiance performance than its predecessor. The data are freely available at <https://disc.gsfc.nasa.gov/datasets/project=MERRA-2>.

#### G. ERA-5

ERA5 is the fifth-generation atmospheric reanalysis model developed by the European Centre for Medium-Range Weather Forecasts (ECMWF), covering the period from January 1940 to the present. This model provides hourly estimates of numerous climate variables, including atmospheric, terrestrial, and oceanic aspects. The data are presented on a horizontal grid of 30 km, and the atmosphere is binned using 137 levels ranging from the Earth's surface to an altitude of

TABLE III  
SUMMARY OF MODELS USED

Model	Availability	Temporal Resolution (min)	Coverage Area
Heliosat-4	2004 to present	1,15,30,60	-66° to 66° in both latitude and longitude
NSRDB	2019 to 2023	10,30,60	all region
DSR	2020 to present	60	all region
LSA-SAF	2004 to present	15	all region
MERRA-2	1980 to present	60	all region
ERA-5	1940 to present	60	all region
GOES-16 Images	2017 to present	15, 10 from 2020	all region

80 km [47]. The model is based on the Integrated Forecasting System (IFS) Cy41r2, which was operational until 2016. Thus, ERA5 benefits from a decade of advances in model physics, core dynamics, and data assimilation compared to the previous ERA-Interim data set. In addition to a significantly improved horizontal resolution of  $0.25^\circ$  latitude ( $31$  km), ERA5 provides hourly output. This model combines satellite and in-situ observations in its estimates using advanced modeling and data assimilation techniques; therefore, ERA5 has been shown to produce more accurate simulations compared to previous generations [48], [49]. The data are freely available at <https://cds.climate.copernicus.eu/datasets/reanalysis-era5-single-levels?tab=download>.

#### H. Models Summary

Table III summarizes the characteristics of the models used in this study, which are available for the region.

### IV. METHODS

The various available estimates are validated against ground measurements from both sites at different time bases, ranging from the native frequency of each model to sixty minutes (one hour). This requires temporal integration of ground measurements and model estimates originally obtained at intra-hourly frequency (Heliosat-4, NSRDB, LSA-SAF, G-CIM). This section describes the data processing and performance metrics used for the evaluation.

### A. Performance Metrics

The most common performance indicators in the field of solar resource assessment have been covered by Ref. [50]; these include the Mean Bias Error (MBE), Mean Absolute Error (MAE), Root Mean Square Error (RMSE), Kolmogorov-Smirnov Integral (KSI), and the statistic proposed by Taylor, known as the Taylor Skill Score (SS4). The first three metrics are defined as follows,

$$\text{MBE} = \frac{\sum_{i=1}^n (y_i - x_i)}{n}, \quad (2)$$

$$\text{MAE} = \frac{\sum_{i=1}^n |y_i - x_i|}{n}, \quad (3)$$

$$\text{RMSE} = \sqrt{\frac{1}{n} \sum_{i=1}^n (y_i - x_i)^2}, \quad (4)$$

where  $x$  and  $y$  are the measured and estimated values, respectively, and  $n$  is the sample size. The MBE measures the systematic bias that a model can introduce in a long-term evaluation, while the MAE and RMSE measure the dispersion of the error using absolute and quadratic norms, respectively. Because of its greater sensitivity to outliers, the RMSE is often used in this area. Both dispersion metrics are reported here for completeness. The three indicators are presented in relative terms as a percentage of the mean of the measured values, referred to here as MBE (%), MAE (%), RMSE (%).

The KSI, defined in Ref. [51], measures the statistical similarity between the measured and estimated values. It is calculated with the equation (5) by integrating the absolute difference between the two empirical cumulative probability functions ( $F_x$  for  $x$  and  $F_y$  for  $y$ ) over the entire range of the target variable (in this case the GHI, denoted as  $z$  in the equation for mathematical purposes). This provides a negatively oriented metric (the lower, the better) that quantifies the statistical difference between the two data sets. Typically, a low RMSE results in a low KSI, although they formally measure different aspects of estimated performance.

$$\text{KSI} = \int |F_x(z) - F_y(z)| dz \quad (5)$$

Finally, the SS4 metric [52] is a statistical measure that evaluates the overall performance of a model, taking into account both the standard deviation and the correlation. In this way, it balances the amplitude of the model's variation relative to the observations and the strength of the linear relationship between the two signals being compared. The SS4 values range from [0,1], with higher values indicating a better performing model and lower values indicating poorer performance. It is calculated as follows:

$$\text{SS4} = \frac{(1 + \rho)^4}{4(\sigma_r + 1/\sigma_r)^2}, \quad (6)$$

with

$$\sigma_r = \frac{\sigma_y}{\sigma_x} \quad \text{and} \quad \rho = \sqrt{\frac{(1/n) \sum_{i=1}^n (y_i - \bar{y})(x_i - \bar{x})}{\sigma_x \sigma_y}} \quad (7)$$

where  $\sigma_x$  and  $\sigma_y$ , and  $\bar{x}$  and  $\bar{y}$  are the standard deviation and the mean value of  $x$  and  $y$ , respectively.

### V. RESULTS

The performance results are presented in Table IV. Performance metrics are reported at 10-minute, 15-minute and/or hourly time bases, depending on the original time scale of each model. Models with higher time resolution can be evaluated at the lower time resolutions. In this case, the higher time base is given by the NSRDB and G-CIM models, which provide estimates at 10-minute granularity. These models can be upscaled to 15 minutes and 1 hour and can therefore be evaluated at all time scales. CAMS and LSA-SAF estimates are originally at 15 minute granularity and are thus evaluated at this and hourly resolutions. All models are evaluated on an hourly time base, which is a common basis for all models and a relevant use case for solar energy applications.

At the 10-minute scale in SA, NSRDB shows a lower mean absolute error (MAE = 15.8% vs. 17.1%) and a better alignment with the actual data distribution as measured by the Kolmogorov-Smirnov Integral (KSI = 5.0 vs. 12.7). However, G-CIM achieves a lower root mean square error (RMSE = 23.4% vs. 26.6%) and a slightly higher skill score (SS4 = 0.84 vs. 0.83), indicating less error dispersion. In LQ, both models exhibit low and comparable bias (MBE = 0.8% vs. 0.9%). NSRDB maintains a lower MAE (11.2% vs. 12.1%) and a better KSI (2.9 vs. 5.3), while G-CIM has a slightly lower RMSE (19.3% vs. 19.9%). Since both models achieve the same SS4 in LQ (0.85), their overall performance in this site is similar. Overall, NSRDB excels in terms of lower absolute error and better distribution fit, while G-CIM offers lower error dispersion. The choice between the two depends on the preferred metric for a given application. However, some practical considerations should be taken into account. NSRDB estimates can be downloaded directly from its web portal, making it readily accessible, whereas G-CIM requires retrieval of GOES-16 products and construction of the model. On the other hand, NSRDB is not an operational model and its estimates for Latin America are not regularly updated. This offers a space for G-CIM application, as once calibrated and locally implemented, its availability depends solely on access to GOES-16 imagery, making it a viable option for real-time applications. Fig. 1 shows a scatter plot of the G-CIM estimates against the measurements at the 10 minute time scale for the SA (top) and LQ (bottom) sites, with the data concentration shown in colour. It can be seen that the higher concentration is around the  $x = y$  diagonal, while larger deviations are less frequent.

The results for these two models (NSRDB and G-CIM) at the 15-minute time scale are very similar to those obtained at the 10-minute time scale. Their relative ranking for each metric and their qualitative assessment are the same. For both sites (SA and LQ) the NSRDB has the lowest mean absolute error (MAE = 15.2% and 10.9% respectively), the best fit to the actual data distribution (KSI = 5.1 and 2.5) and the highest skill score (SS4 = 0.85 and 0.87). G-CIM again has the lowest RMSE (23.0% and 18.1% for SA and LQ respectively) and a higher KSI (12.5 and 4.9) compared to NSRDB. The additional models on this time scale (CAMS and LSA-SAF) do not provide better performance on any metric. CAMS and

TABLE IV  
MULTI-SCALE PERFORMANCE ASSESSMENT. THE MEAN VALUE OF THE NORMALIZATION FOR THE MBE, THE MAE AND THE RMSE IS OF 480 W/m<sup>2</sup> FOR SA AND OF 623.1 W/m<sup>2</sup> FOR LQ

Model	SA					LQ				
	MBE(%)	MAE(%)	RMSE(%)	KSI	SS4	MBE(%)	MAE(%)	RMSE(%)	KSI	SS4
60 min										
NSRDB	-3.6	<b>12.4</b>	<b>19.7</b>	<b>5.1</b>	<b>0.89</b>	<b>0.8</b>	<b>7.8</b>	<b>12.6</b>	<b>1.7</b>	<b>0.93</b>
G-CIM	5.4	15.8	20.7	11.9	<b>0.89</b>	0.8	9	13.2	3.8	0.92
CAMS	-5.1	17.2	25.4	4.8	0.86	-9.1	15.1	23.3	9.1	0.83
LSA-SAF	9.3	18	27.5	10.2	0.83	3.2	10.9	19.4	3.5	0.85
MERRA-2	31.5	34.8	51.1	31.5	0.64	$\simeq 0$	13.6	22	2.5	0.80
ERA-5	4.1	21.1	31.6	9.8	0.74	-3.9	13.7	22.2	4.6	0.80
DSR	<b>1.3</b>	19.9	27.5	10.2	0.83	-2.9	17.1	22.5	6.5	0.78
15 min										
NSRDB	<b>-4.2</b>	<b>15.2</b>	25.3	<b>5.1</b>	<b>0.85</b>	<b>0.8</b>	<b>10.9</b>	18.5	<b>2.5</b>	<b>0.87</b>
G-CIM	4.9	16.8	<b>23</b>	12.5	0.84	<b>0.8</b>	11.6	<b>18.1</b>	4.9	<b>0.87</b>
CAMS	-4.9	19.5	29.3	5.1	0.81	-9.1	17.3	27.4	9.1	0.77
LSA-SAF	9.5	20.1	31.4	11.2	0.78	3.3	13.2	24	4.5	0.79
10 min										
NSRDB	<b>-4.2</b>	<b>15.8</b>	26.6	<b>5</b>	0.83	<b>0.8</b>	<b>11.2</b>	19.9	<b>2.9</b>	<b>0.85</b>
G-CIM	4.8	17.1	<b>23.4</b>	12.7	<b>0.84</b>	0.9	12.1	<b>19.3</b>	5.3	<b>0.85</b>

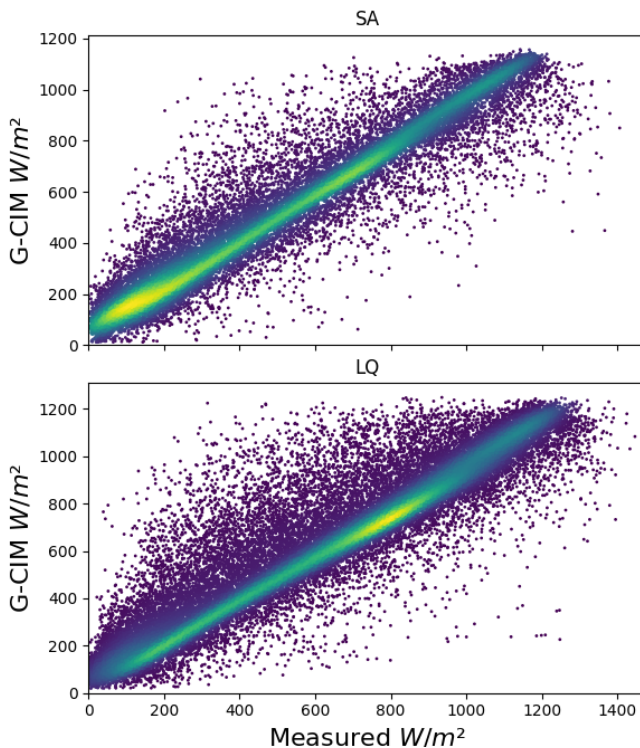


Fig. 1. Scatter plots of the G-CIM model estimates versus measurements at 10 minute resolution. (bottom) Salta (SA); (down) La Quiaca (LQ).

LSA-SAF generally have a higher bias than NSRDB and G-CIM at both sites, with the exception of the CAMS model at SA, whose bias is similar to the previous two (MBE = -4.9% vs. -4.2% of NSRDB and 4.9% of G-CIM). The CAMS has the highest bias in LQ (MBE = -9.1%), while the LSA-SAF has the highest bias in SA (MBE = 9.5%). In SA, the CAMS estimates perform better than the LSA-SAF for all indicators. However, for LQ the situation is exactly the opposite. In both locations, CAMS and LSA-SAF show worse performance than NSRDB and G-CIM on a 15 minute time scale, with higher performance metrics and lower skill scores.

On an hourly time scale, the seven models can be compared. The NSRDB shows the best performance for almost all metrics at both sites, the only exception being the MBE at SA, for which the DSR estimates show the lowest values (MBE = 1.3%). For most models, the MBE is between  $\pm 5.5\%$ , with the exception of the LSA-SAF satellite model and the MERRA-2 reanalysis data. Notably, the ERA-5 reanalysis data is also in this range with a bias of 4.1%, which is comparable to that of the best performing satellite-based models. The MERRA-2 estimates are largely biased in SA (MBE = 31.5%) and almost unbiased in LQ (MBE  $\simeq 0$ ), which is a rather unusual situation. This suggests a significant problem with the cloud representation by this model, so that it performs much better in a mostly clear site (LQ) than in a mixed site (SA) where clear and cloudy skies alternate. Based on the MAE, RMSE and SS4 values, three and two groups of models can be displayed in SA and LQ respectively. In SA, the first group is made by the



NSRDB and G-CIM with MAE between 12.4% and 15.8% and RMSE between 19.7% and 20.7%, and the best SS4 (0.89). In the second group (CAMS, LSA-SAF, DSR) the MAE ranges from 17.2% to 19.9%, RMSE from 25.4% to 27.5%, and SS4 from 0.83 to 0.86. The third group is made by the reanalysis datasets in which MAE is between 21.1% and 34.8%, RMSE between 31.6% and 51.1%, and SS4 between 0.74 and 0.64. The two groups at LQ can be formed by {NSRDB, G-CIM, LSA-SAF} and {CAMS, MERRA-2, ERA-5, DSR}. In the first group MAE ranges from 7.8% to 10.9%, RMSE from 12.6% to 19.4%, and SS4 from 0.85 to 0.93, while in the second group MAE is between 13.6% and 17.1%, RMSE between 22.0% and 23.3%, and SS4 between 0.83 and 0.78. The KSI reveals different ability of the models to represent data distribution. In SA, the best models from this metric's view are the CAMS (4.8) and NSRDB (5.1). In LQ most models display low value of this metric, and 4 models can be identified as best performing in this sense, being NSRDB (1.7), MERRA-2 (2.5), LSA-SAF (3.5) and G-CIM (3.8). Overall, NSRDB is the best-performing model at this time scale in both locations and G-CIM remains a substantial alternative, very close in performance. CAMS and LSA-SAF demonstrate moderate performance, while MERRA-2, ERA-5, and DSR show significantly higher errors and lower skill scores, making them less suitable for high-accuracy applications.

## VI. DISCUSSION

The presented results show that the G-CIM and NSRDB models have the best performance among all evaluated models across the different time scales. Both models are based on images derived from the GOES-16 satellite, as is the DSR model. However, it is important to note that the DSR model has a temporal resolution of 60 minutes and an approximate spatial resolution of 55 km, in contrast to the 10 minute temporal and  $4 \times 4$  km spatial resolutions of G-CIM and NSRDB, respectively. This highlights the relationship between model performance and temporal and spatial resolution, although DSR modelling and reduced input information may also have an effect. For the sites studied, the performance of the DSR model is similar to that of reanalysis models such as ERA-5 and MERRA-2, a trend also reported in a separate evaluation carried out at two sites in Uruguay [53]. In addition, CAMS and LSA-SAF in SA report performance metrics similar to those found in Refs. [20], [54]. In particular, Ref. [54] indicates that CAMS performs poorly at a site approximately 55 km northwest of the SA station.

Regarding the performance of the reanalysis data sets ERA-5 and MERRA-2 in LQ, the former shows a slight negative bias, while latter shows no bias. However, both models perform similarly in terms of mean absolute error and root mean square error. This suggests that although MERRA-2 does not have an average bias, it still produces significant deviations. Therefore, if the objective is to avoid average bias, MERRA-2 appears to be more suitable than ERA-5 at this location. Conversely, the MERRA-2 model shows the least appropriate performance in SA. This issue is probably related to the spatial resolution of the models. The SA station is located with

several microclimates separated by less than 40 km, which undoubtedly affects the performance of the solar irradiance modelled data. In any case, large RMSE values are found at SA for both reanalysis datasets and CAMS and DSR satellite estimates, indicating deficiencies in cloud retrieval due to pixel size and viewing angle for satellite models and pixel size and modelling for reanalysis.

As shown in Refs. [11], [18], [25], the use of a CIM strategy based on GOES imagery with local adjustment is one of the best options for estimating the GHI. In this work, the G-CIM performance metrics are competitive with those of the NSRDB, the best performing model. Considering that the NSRDB model includes fine physical modelling and also uses the GOES-16 images at the same time rate (10 minutes), it can be concluded that the simple G-CIM model performs quite well. Furthermore, its performance is within the expected ranges according to the literature [12], close to the best. It should also be noted that the performance of the NSRDB model in LQ shows a lower performance compared to other desert sites [10], which could be due to a more complex ground albedo terrain.

### A. Performance as a Function of Time Scale

Fig. 2 shows the RMSE performance of all models at different time scales. The colours of the bars indicate different models. It can be seen that the RMSE decreases with increasing time scale, as is clear for the green models (NSRDB and G-CIM), the dark blue model (CAMS) and the salmon pink model (LSA-SAF). As expected, the reduction is more pronounced from 15 minutes to 1 hour than from 10 minutes to 15 minutes. The same increase in metrics with time scale can be seen in Table IV for MAE and SS4. This effect is related to the temporal variability of solar radiation at the different time scales, which is greater at higher time resolution and therefore more difficult to model. In contrast, the KSI metric is more stable between time scales, being almost the same for all time scales in SA and showing a slight decrease from 10 and 15 min to 1 h in LQ.

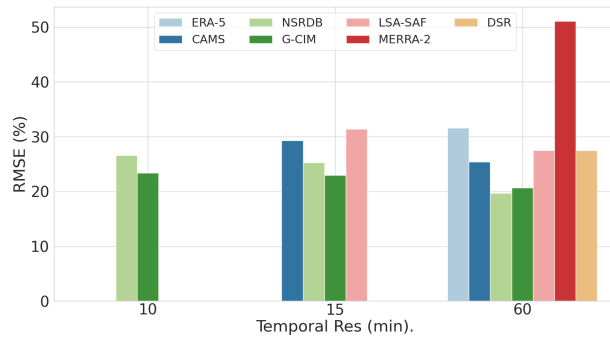
### B. Performance as a Function of the Sun's Zenith Angle

Figs. 3a and 3b show the RMSE of the different models as a function of Solar Zenith Angle (SZA) for the hourly time scale at both sites. It can be observed that the DSR and CAMS models have higher error rates for large SZA values. Although this trend is also present in the other models, it is more significant for DSR and CAMS, being greater than 100%. For DSR, this increase may be directly related to the interpolation used to fill gaps in the model when  $SZA^\circ > 70^\circ$ . In the case of CAMS, the increased error is most likely due to parallax, as the sites are located at an extreme limit of the model coverage area with very large satellite viewing angles, a limitation previously reported in Ref. [25].

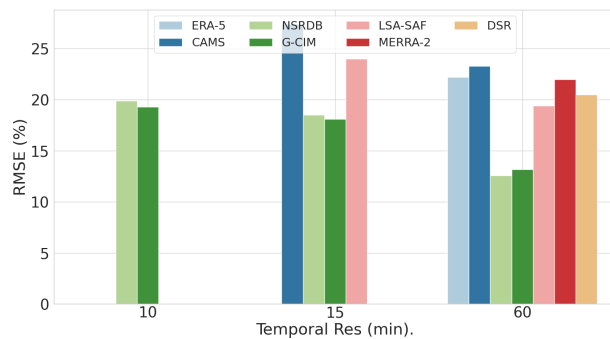
### C. Probability Distribution Analysis

The comparison of probability density distributions for global horizontal irradiance (GHI) is shown in Fig. 4. It

shows the distribution of both the measured data and the G-CIM modelled estimates at temporal resolutions of 10, 15 and 60 minutes from left to right, and for SA (top) and LQ (bottom), illustrating the strengths and limitations of the model at different time scales. At the 10-min resolution, larger discrepancies are evident, particularly at high irradiance levels (above 900 W/m<sup>2</sup>), where G-CIM tends to overestimate the probability density function, resulting in sharper and right-shifted peaks. This behaviour indicates a limited sensitivity of the model to extreme clear sky conditions or rapid intra-day variability, the latter typically associated with intermittent partly cloudy conditions. As the temporal resolution increases to 15 and 60 min, the differences between the modelled and measured distributions decrease. For both stations, the improvement is observed at medium and high irradiance values, while at low irradiance values the agreement is quite good over all time scales. The improvement can be attributed to the smoothing effect of temporal aggregation, which acts as a filter that suppresses short-term fluctuations and emphasises broader statistical patterns. Nevertheless, the reduction in temporal resolution limits the ability of the model to capture short-lived extreme events and is an important limitation for applications requiring high-frequency accuracy.

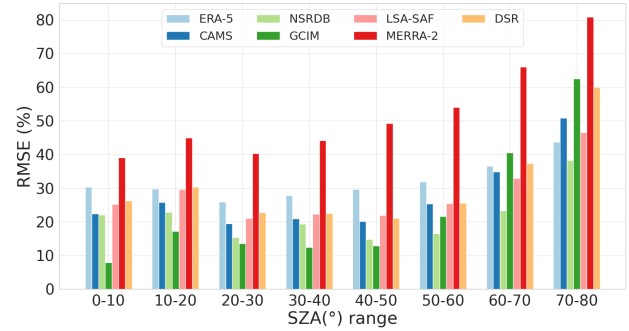


(a) RMSE(%) at different time scales in SA

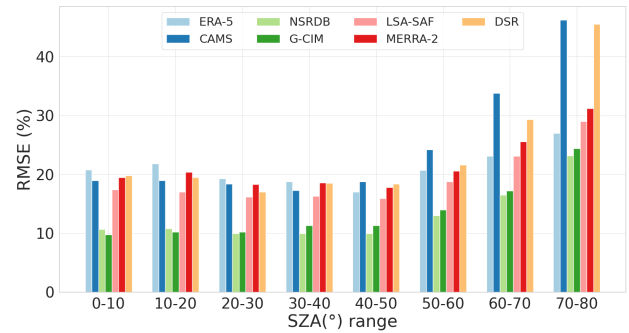


(b) RMSE(%) at different time scales in LQ

Fig. 2. RMSE(%) of the evaluated models at different temporal resolutions. (a) Salta (SA); (b) La Quiaca (LQ)

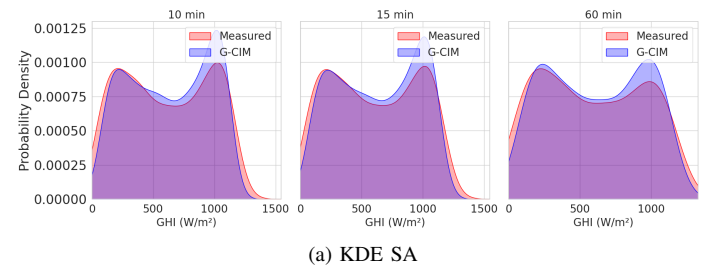


(a) RMSE(%) in SA

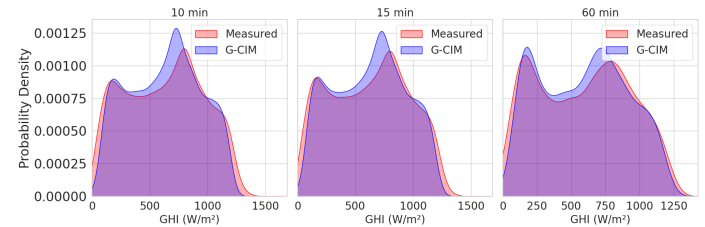


(b) RMSE(%) in LQ

Fig. 3. RMSE(%) of the evaluated models at hourly resolution grouped by SZA ranges. (a) Salta (SA); (b) La Quiaca (LQ)



(a) KDE SA



(b) KDE LQ

Fig. 4. Kernel density estimation (KDE) plots showing the probability density of measurements (red) and G-CIM estimates (blue), evaluated at temporal resolutions of 10, 15, and 60 minutes. (a) Salta (SA); (b) La Quiaca (LQ).

#### D. Other Factors Influencing Uncertainty

The differences in accuracy between the various satellite and reanalysis models evaluated in this work for these two sites can be attributed to several factors, including local climatic



characteristics, altitude, satellite spatial and temporal resolution, and the methods used for cloud retrieval and irradiance estimation.

Salta (SA), a pre-Andean urban site, is characterised by frequent cloud cover due to its location in the Lerma Valley. This makes cloud retrieval more challenging for satellite models, as cloud dynamics and varying surface albedo from the surrounding terrain introduce additional sources of error. In contrast, La Quiaca (LQ), a semi-arid Andean steppe, experiences significantly more sunshine hours and more stable clear sky conditions, making it generally easier for satellite-based models to accurately estimate solar irradiance as long as the cloud-free albedo remains low (e.g. below 25%). Altitude also plays a crucial role, as La Quiaca, at 3,468 m above sea level, has a thinner atmosphere, which reduces scattering and absorption effects. Some models, particularly reanalysis datasets such as MERRA-2 and ERA-5, may not fully account for these altitude effects, leading to discrepancies in irradiance estimates. Meanwhile, Salta, at 1,233 m above sea level, is influenced by complex microclimates and the surrounding topography, which further challenge the accuracy of the models.

Another key factor influencing model performance is spatial and temporal resolution. Models with coarser spatial resolution (e.g. ERA-5, MERRA-2, DSR) tend to perform worse in Salta due to the heterogeneity of its terrain and climatic conditions, while models with higher resolution (e.g. G-CIM and NSRDB) achieve better accuracy by capturing local variations more effectively. Similarly, models with higher temporal resolution, such as NSRDB and G-CIM, which use GOES-16 satellite imagery with updates every 10-15 minutes, outperformed others by better capturing short-term irradiance variations, which is particularly important in regions with frequent cloud variability, such as Salta.

The cloud retrieval methodology and atmospheric inputs also contributed to the differences in accuracy. Reanalysis data (e.g. ERA-5, MERRA-2) showed higher uncertainty at Salta, probably because they rely on global atmospheric models that do not resolve local cloud microphysics or topographic effects in detail. In contrast, G-CIM and NSRDB, which use real-time cloud data from GOES-16 imagery, show superior performance because they rely on actual cloud observations rather than simulated cloud cover from numerical models. However, even these models had some errors, particularly at high solar zenith angles, where satellite-based cloud retrievals tend to be less reliable.

Terrain characteristics and surface albedo also affected model accuracy. Salta's mixed urban and natural landscape results in variable ground reflectivity, which can introduce bias in satellite models, particularly those with coarse pixel resolution. In La Quiaca, the combination of high altitude and high surface reflectivity (resulting from the semi-arid environment and light-coloured terrain) can cause some models to either over- or underestimate irradiance if they do not accurately account for albedo effects.

Overall, it is the combination of the previous factors that explains the performance of the different models. In Salta, the combination of frequent cloud cover, complex terrain reflectivity and lower spatial resolution in some models led

to higher errors, especially for reanalysis-based estimates such as MERRA-2 and ERA-5. Conversely, in La Quiaca, the more stable and higher altitude conditions allowed most models to perform better, although challenges remained for those that did not correctly account for atmospheric transmission and surface albedo effects.

These findings underscore the importance of selecting models that are tailored to regional characteristics. In areas with high cloud variability, such as Salta, satellite-based models with frequent updates (e.g. NSRDB, G-CIM) are preferable, while reanalysis models should be used with caution or require local adaptation. In high altitude, semi-arid environments such as La Quiaca, models that correctly account for altitude-related atmospheric effects and surface reflectivity are essential to minimise bias. In addition, higher spatial resolution and site-specific model calibration are crucial to improve accuracy, especially in regions with microclimatic variations and complex topography.

### *E. Strengths and Limitations of the Study*

This study presents a comprehensive comparative assessment of satellite and reanalysis models for estimating solar irradiance in northwestern Argentina. One of its main strengths is the detailed evaluation of several models, including both satellite and reanalysis-based approaches, under exactly the same conditions, using high quality ground-based measurements from two representative sites in the region. In addition, the models were evaluated at 10, 15 and 60-min time resolutions, allowing a more thorough characterisation of their performance. Another major strength lies in the local adaptation of the models, in particular the implementation of the G-CIM model, which is calibrated using GOES-16 imagery. This approach provides a more reliable reference with improved accuracy compared to global databases. Finally, this study makes a significant contribution to regional knowledge as it is the first comprehensive analysis of its kind in the region, providing critical insights for researchers and professionals in the solar energy sector.

However, the study has some limitations. Firstly, the geographical coverage is limited to two locations (Salta and La Quiaca), which means that the results cannot be generalised to the whole region without further studies in additional locations. Another limitation is the availability of data, as some models, such as the NSRDB, only provide data up to 2023, making it impossible to evaluate up to the present day.

Despite these limitations, the findings of this study provide valuable guidance for selecting appropriate models for solar resource assessment in northwestern Argentina. Future research could extend this analysis by including additional measurement sites and exploring correction methods to improve the accuracy of lower performing models.

## VII. CONCLUSIONS

A benchmark study was conducted on solar irradiation data sources at various sub-hourly scales for Northwest Argentina, where seven modeled data sources—including different satellite-based schemes and two reanalysis datasets—were

evaluated using two years of high-quality, ground-based measurements from two climatically distinct sites. The semi-empirical G-CIM model, locally adjusted and based on GOES-East satellite images, proved to be the most accurate option, demonstrating superior overall metrics and spatial consistency. In particular, at the 10-minute scale in Salta, G-CIM yielded an RMSD of 23.4% with a mean bias of 4.8%, compared to NSRDB's RMSD of 26.6% and bias of -4.2%. At the 60-minute scale, NSRDB and G-CIM in Salta reported RMSDs of 19.7% and 20.7% (with biases of -3.6% and 5.4%, respectively), while both models achieved RMSD values below 20% and mean biases under 1% in La Quiaca. NSRDB estimates also exhibited strong overall performance. In contrast, the MERRA-2 reanalysis data showed significant uncertainties in the Salta region—with a bias reaching 31.5% and RMSE up to 51.1%—indicating that its use in such complex microclimatic conditions is not recommended without rigorous post-processing based on high-quality measurements. Conversely, in La Quiaca, MERRA-2 demonstrated performance comparable to other models, although the superior temporal and spatial resolution of GOES-16-based models (G-CIM and NSRDB) resulted in notably better performance.

The significant differences in model accuracy between the two sites are directly related to climatic variability and resolution issues. In Salta, where several microclimates exist within a 40 km radius, factors such as cloud retrieval accuracy and pixel size are critical. For solar energy applications where uncertainty is a key concern, G-CIM and NSRDB are recommended. In contrast, the reanalysis models, particularly MERRA-2 and ERA-5, generally show weaker performance in these complex environments and should only be used when supplemented by appropriate site-adaptation procedures.

This study, which is the first of its kind in Latin America, fills a critical gap in the literature and provides industry professionals with quantitative insights—such as RMSD values ranging from 12.6% to 26.6% and mean biases from under 1% to as high as 31.5%—to assess the applicability of different irradiance estimation models for solar energy projects in the region.

## REFERENCES

- [1] M. Schnitzer, C. Thuman, and P. Johnson, "The impact of solar uncertainty on project financeability: mitigating energy risk through on-site monitoring," *Proceedings of the American Solar Energy Society (ASES)*, pp. 1–5, 2012.
- [2] A. McMahan, C. Grover, and F. Vignola, "Evaluation of resource risk in solar-project financing," *Solar Energy Forecasting and Resource Assessment*, pp. 81–95, 07 2013. Available: <https://doi.org/10.1016/B978-0-12-397177-7.00004-8>.
- [3] R. Perez, R. Seals, and A. Zelenka, "Comparing satellite remote sensing and ground network measurements for the production of site/time specific irradiance data," *Solar Energy*, vol. 60, no. 2, pp. 89–96, 1997. Available: <https://doi.org/10.1023/A:1008202821328>.
- [4] A. Zelenka, R. Perez, R. Seals, and D. Renné, "Effective accuracy of satellite-derived hourly irradiances," *Theoretical and Applied Climatology*, vol. 62, no. 3, pp. 199–207, 1999. Available: <https://doi.org/10.1023/A:1008202821328>.
- [5] T. Huld, R. Müller, and A. Gambardella, "A new solar radiation database for estimating pv performance in europe and africa," *Solar Energy*, vol. 86, no. 6, pp. 1803–1815, 2012. Available: <https://doi.org/10.1016/j.solener.2012.03.006>.
- [6] C. Vernay, S. Pitaval, and P. Blanc, "Review of satellite-based surface solar irradiation databases for the engineering, the financing and the operating of photovoltaic systems," *Energy Procedia*, vol. 57, pp. 1383–1391, 2014. Available: <https://doi.org/10.1016/j.egypro.2014.10.129>.
- [7] M. Marchand, A. Ghennioui, E. Wey, and L. Wald, "Comparison of several satellite-derived databases of surface solar radiation against ground measurement in morocco," *Advances in Science and Research*, vol. 15, pp. 21–29, 2018. Available: <https://doi.org/10.5194/asr-15-21-2018>.
- [8] M. C. Bueso, J. M. Paredes-Parra, A. Mateo-Aroca, and A. Molina-García, "A characterization of metrics for comparing satellite-based and ground-measured global horizontal irradiance data: A principal component analysis application," *Sustainability*, vol. 12, no. 6, 2020. Available: <https://doi.org/10.3390/su12062454>.
- [9] G. Salazar, C. Gueymard, J. Galdino, O. Vilela, and N. Fraidenraich, "Solar irradiance time series derived from high-quality measurements, satellite-based models, and reanalyses at a near-equatorial site in Brazil," *Renewable and Sustainable Energy Reviews*, vol. 117, p. 109478, 01 2020. Available: <https://doi.org/10.1016/j.rser.2019.109478>.
- [10] A. S. Altamirano, R. Calleja, R. Alonso-Suárez, and R. Cabanillas-López, "Uncertainty assessment of satellite-based solar radiation data in the southeastern sonoran desert," in *2024 IEEE 52nd Photovoltaic Specialist Conference (PVSC)*, pp. 1008–1014, 2024. Available: <https://doi.org/10.1109/PVSC57443.2024.10749660>.
- [11] I. Sarazola, A. Laguarda, J. C. Ceballos, and R. Alonso-Suárez, "Benchmarking of modeled solar irradiation data in Uruguay at a daily time scale," *IEEE Latin America Transactions*, vol. 21, p. 1040–1048, Aug. 2023. Available: <https://doi.org/10.1109/TLA.2023.10251811>.
- [12] D. Yang and J. Bright, "Worldwide validation of 8 satellite-derived and reanalysis solar radiation products: A preliminary evaluation and overall metrics for hourly data over 27 years," *Solar Energy*, vol. 210, pp. 3–19, 2020. Available: <https://doi.org/10.1016/j.solener.2020.04.016>.
- [13] C. Gueymard, "Solar radiation resource: measurement, modeling, and methods," in *Comprehensive Renewable Energy* (T. Letcher, ed.), pp. 176–212, Oxford: Elsevier, second ed., 2022. Available: <https://doi.org/10.1016/B978-0-12-819727-1.00101-1>.
- [14] G. Huang, Z. Li, X. Li, S. Liang, K. Yang, D. Wang, and Y. Zhang, "Estimating surface solar irradiance from satellites: Past, present, and future perspectives," *Remote Sensing of Environment*, vol. 233, p. 111371, 2019. Available: <https://doi.org/10.1016/j.rse.2019.111371>.
- [15] R. Perez, P. Ineichen, K. Moore, M. Kmiecik, C. Chain, R. George, F., and Vignola, "A new operational model for satellite-derived irradiances: description and validation," *Solar Energy*, vol. 73, pp. 307–317, 2002. Available: [https://doi.org/10.1016/S0038-092X\(02\)00122-6](https://doi.org/10.1016/S0038-092X(02)00122-6).
- [16] Z. Q. et al., "Fast radiative transfer parameterisation for assessing the surface solar irradiance: the Heliosat-4 method," *Meteorologische Zeitschrift*, vol. 26, pp. 33–57, 02 2017. Available: <https://doi.org/10.1127/metz/2016/0781>.
- [17] A. Laguarda, G. Giacosa, R. Alonso-Suárez, and G. Abal, "Performance of the site-adapted CAMS database and locally adjusted cloud index models for estimating global solar horizontal irradiation over the Pampa Húmeda," *Solar Energy*, vol. 199, pp. 295–307, 2020. Available: <https://doi.org/10.1016/j.solener.2020.02.005>.
- [18] R. D. Ledesma, G. A. Salazar, and O. de Castro Vilela, "Avances en la estimación de irradiancia solar en las provincias de Salta y Jujuy mediante imágenes satelitales GOES-16," *Avances en Energías Renovables y Medio Ambiente (AVERMA)*, 2023. Available: <https://doi.org/2796-8111>.
- [19] G. A. Salazar, R. Alonso-Suárez, A. Laguarda Cirigliano, and R. D. Ledesma, "Evaluación del proceso de adaptación al sitio aplicado a la irradiancia solar global medida en la ciudad de Salta, Argentina," *Avances en Energías Renovables y Medio Ambiente - AVERMA*, vol. 25, p. 353–362, may 2022. DOI: 2796-8111.
- [20] N. Sarmiento, S. Belmonte, P. Dellicompagni, J. Franco, K. Escalante, and J. Sarmiento, "A solar irradiation GIS as decision support tool for the Province of Salta, Argentina," *Renewable Energy*, vol. 132, pp. 68–80, 2019. Available: <https://doi.org/10.1016/j.renene.2018.07.081>.
- [21] M. Peel, B. Finlayson, and T. McMahon, "Updated world map of the Köppen-Geiger climate classification," *Hydrology and Earth System Sciences Discussions*, vol. 11, pp. 1633–1644, 2007. Available: <https://doi.org/10.5194/hess-11-1633-2007>.
- [22] F. M. Nollas, G. A. Salazar, and C. A. Gueymard, "Quality control procedure for 1-minute pyranometric measurements of global and shadowband-based diffuse solar irradiance," *Renewable Energy*, vol. 202, pp. 40–55, 2023. Available: <https://doi.org/10.1016/j.renene.2022.11.056>.
- [23] D. M. Hawkins, "Testing a sequence of observations for a shift in location," *Journal of the American Statistical Association*, vol. 72, no. 357, pp. 180–186, 1977. Available: <https://doi.org/10.2307/2286934>.

- [24] R. Perez, P. Ineichen, K. Moore, M. Kmiecik, C. Chain, R. George, and F. Vignola, "A new operational model for satellite-derived irradiances description and validation," *Solar Energy*, vol. 73, pp. 307–317, 11 2002. Available: <https://doi.org/10.1023/A:1008202821328>.
- [25] A. Laguarda, G. Giacosa, R. Alonso-Suárez, and G. Abal, "Performance of the site-adapted CAMS database and locally adjusted cloud index models for estimating global solar horizontal irradiation over the Pampa Húmeda," *Solar Energy*, vol. 199, pp. 295–307, 2020. Available: <https://doi.org/10.1016/j.solener.2020.02.005>.
- [26] Z. Qu et al., "Fast radiative transfer parameterisation for assessing the surface solar irradiance: The Heliosat-4 method," *Meteorologische Zeitschrift*, vol. 26, pp. 33–57, 02 2017. Available: <https://doi.org/10.1127/metz/2016/0781>.
- [27] B. Mayer and A. Kylling, "Technical note: The libradtran software package for radiative transfer calculations - description and examples of use," *Atmospheric Chemistry and Physics*, vol. 5, no. 7, pp. 1855–1877, 2005. Available: <https://doi.org/10.5194/acp-5-1855-2005>.
- [28] M. K. K. T. Kriebel, G. Gesell and H. Mannstein, "The cloud analysis tool apollo: Improvements and validations," *International Journal of Remote Sensing*, vol. 24, no. 12, pp. 2389–2408, 2003. Available: <https://doi.org/10.1080/01431160210163065>.
- [29] M. Sengupta, Y. Xie, A. Lopez, A. Habte, G. Maclaurin, and J. Shelby, "The National Solar Radiation Data Base (NSRDB)," *Renewable and sustainable energy reviews*, vol. 89, pp. 51–60, 2018. Available: <https://doi.org/10.1016/j.rser.2018.03.003>.
- [30] Y. Xie, M. Sengupta, and J. Dudhia, "A fast all-sky radiation model for solar applications (FARMS): Algorithm and performance evaluation," *Solar Energy*, vol. 135, pp. 435–445, 2016. Available: <https://doi.org/10.1016/j.solener.2016.06.003>.
- [31] I. Laszlo, H.-Y. Kim, and H. Liu, *Algorithm Theoretical Basis Document For Downward Shortwave Radiation (Surface), and Reflected Shortwave Radiation (TOA), Enterprise Processing System (EPS) Version*. NOAA/NESDIS/STAR, 2020.
- [32] D. Rutan, S. Kato, D. Doelling, F. Rose, L. Nguyen, T. Caldwell, and N. Loeb, "CERES synoptic product: Methodology and validation of surface radiant flux," *Journal of Atmospheric and Oceanic Technology*, vol. 32, no. 6, pp. 1121 – 1143, 2015. Available: <https://doi.org/10.1023/A:1008202821328>.
- [33] D. Fillmore, D. Rutan, S. Kato, F. Rose, and T. Caldwell, "Evaluation of aerosol optical depths and clear-sky radiative fluxes of the CERES Edition 4.1 SYN1deg data product," *Atmospheric Chemistry and Physics*, vol. 22, no. 15, pp. 10115–10137, 2022. Available: <https://doi.org/10.1023/A:1008202821328>.
- [34] R. Alonso-Suárez, *Estimación del recurso solar en Uruguay mediante imágenes satelitales. Tesis de doctorado. Universidad de la República (Uruguay)*. PhD thesis, Universidad de la República (Uruguay). Facultad de Ingeniería., 2017. Available: <https://doi.org/10.1023/A:1008202821328>.
- [35] M. Derrien and H. L. Gléau, "MSG/SEVIRI cloud mask and type from SAFNWC," *International Journal of Remote Sensing*, vol. 26, no. 21, pp. 4707–4732, 2005. Available: <https://doi.org/10.1080/01431160500166128>.
- [36] N. SAF, "User manual for the cloud product processors of the nwc/geo: Science part," tech. rep., Météo-France / Centre d'études en Météorologie Satellitaire, 2022.
- [37] X. Ceamanos, D. Carrer, and J.-L. Roujean, "Improved retrieval of direct and diffuse downwelling surface shortwave flux in cloudless atmosphere using dynamic estimates of aerosol content and type: application to the LSA-SAF project," *Atmospheric Chemistry and Physics*, vol. 14, no. 15, pp. 8209–8232, 2014. Available: <https://doi.org/10.5194/acp-14-8209-2014>.
- [38] B. Geiger, C. Meurey, D. Lajas, L. Franchistéguy, D. Carrer, and J.-L. Roujean, "Near real-time provision of downwelling shortwave radiation estimates derived from satellite observations," *Meteorological Applications*, vol. 15, no. 3, pp. 411–420, 2008. Available: <https://doi.org/10.1002/met.84>.
- [39] R. D. Ledesma, G. A. Salazar, and O. de Castro Vilela, "ARGP-V2: un modelo práctico para la estimación de irradiancia global horizontal en condiciones de cielo claro para sitios de altura," *Avances en Energías Renovables y Medio Ambiente (AVERMA)*, 2022. DOI: 2796-8111.
- [40] D. Cano, J. Monget, M. Albuissou, H. Guillard, N. Regas, and L. Wald, "A method for the determination of the global solar radiation from meteorological satellite data," *Solar Energy*, vol. 37, no. 1, pp. 31–39, 1986. Available: <https://doi.org/10.1023/A:1008202821328>.
- [41] A. Laguarda, G. Abal, and R. Alonso-Suárez, "Modelo semi-empírico simple de irradiación solar global a partir de imágenes satelitales GOES," in *Anais Congresso Brasileiro de Energia Solar-CBENS*, 2018. Available: <https://doi.org/10.59627/cbens.2018.707>.
- [42] R. Gelaro et al., "The Modern-Era Retrospective Analysis for Research and Applications, Version 2 (MERRA-2)," *Journal of Climate*, vol. 30, no. 14, pp. 5419–5454, 2017. Available: <https://doi.org/10.1175/JCLI-D-16-0758.1>.
- [43] M. Rienecker, *The GEOS-5 data assimilation system: documentation of versions 5.0.1, 5.1.0, and 5.2.0*. NASA technical memorandum, National Aeronautics and Space Administration, Goddard Space Flight Center, 2008.
- [44] A. Molod, L. Takacs, M. Suárez, and J. Bacmeister, "Development of the GEOS-5 atmospheric general circulation model: Evolution from MERRA to MERRA2," *Geoscientific Model Development*, vol. 8, pp. 1339–1356, 2015.
- [45] M. Rienecker et al., "MERRA: NASA's Modern-Era Retrospective Analysis for Research and Applications," *Journal of Climate*, vol. 24, no. 14, pp. 3624–3648, 2011. Available: <https://doi.org/10.1175/JCLI-D-11-00015.1>.
- [46] F. Feng and K. Wang, "Does the modern-era retrospective analysis for research and applications-2 aerosol reanalysis introduce an improvement in the simulation of surface solar radiation over China?," *International Journal of Climatology*, vol. 39, pp. 1305–1318, 10 2018. Available: <https://doi.org/10.1002/joc.5881>.
- [47] H. Hersbach et al., "The era5 global reanalysis," *Quarterly Journal of the Royal Meteorological Society*, vol. 146, no. 730, pp. 1999–2049, 2020. Available: <https://doi.org/10.1023/A:1008202821328>.
- [48] L. Hoffmann, G. Günther, D. Li, O. Stein, X. Wu, S. Griessbach, Y. Heng, P. Konopka, R. Müller, B. Vogel, and J. S. Wright, "From era-interim to era5: the considerable impact of ecmwf's next-generation reanalysis on lagrangian transport simulations," *Atmospheric Chemistry and Physics*, vol. 19, no. 5, pp. 3097–3124, 2019. Available: <https://doi.org/10.1023/A:1008202821328>.
- [49] M. Nogueira, "Inter-comparison of era-5, era-interim and gpcp rainfall over the last 40 years: Process-based analysis of systematic and random differences," *Journal of Hydrology*, vol. 583, p. 124632, 2020. Available: <https://doi.org/10.1023/A:1008202821328>.
- [50] J. Zhang, A. Florita, B.-M. Hodge, S. Lu, H. F. Hamann, V. Banunarayanan, and A. M. Brockway, "A suite of metrics for assessing the performance of solar power forecasting," *Solar Energy*, vol. 111, pp. 157–175, 2015. Available: <https://doi.org/10.1016/j.solener.2014.10.016>.
- [51] B. Espinar, L. Ramírez, A. Drews, H. G. Beyer, L. F. Zarzalejo, J. Polo, and L. Martín, "Analysis of different comparison parameters applied to solar radiation data from satellite and german radiometric stations," *Solar Energy*, vol. 83, no. 1, pp. 118–125, 2009. Available: <https://doi.org/10.1016/j.solener.2008.07.009>.
- [52] A. H. Murphy and E. S. Epstein, "Skill scores and correlation coefficients in model verification," *Monthly Weather Review*, vol. 117, no. 3, pp. 572 – 582, 1989. Available: [https://doi.org/10.1175/1520-0493\(1989\)117<0572:SSACCI>2.0.CO;2](https://doi.org/10.1175/1520-0493(1989)117<0572:SSACCI>2.0.CO;2).
- [53] R. Ledesma, R. Alonso-Suárez, A. Monetta, A. Laguarda, O. Vilela, and G. Salazar, "Evaluación en uruguay del producto dsr goes-16 de irradiancia solar global horizontal," *Avances en Energías Renovables y Medio Ambiente (AVERMA)*, 2023. DOI: 2796-8111.
- [54] D. Rodrigues de Miranda, J. V. de Medeiros, O. Vilela, N. Fraidenraich, and G. Salazar, "Simulación de generación de módulo FV en la ciudad de Salta utilizando valores estadísticamente representativos de radiación solar y temperatura adaptados de bases de datos satelitales," in *Avances en Energías Renovables y Medio Ambiente*, vol. 26, pp. 335–343, 2022. DOI: 2796-8111.



**Rubén Ledesma** holds a Bachelor's degree in Systems Analysis and is pursuing a Doctorate in Science with a focus on renewable energies at the National University of Salta. He currently serves as a fellow at CONICET, stationed at the Non-Conventional Energy Research Institute (INENCO). His research interests revolve around satellite-based solar resource estimation and the application of machine learning techniques in this domain.



**Rodrigo Alonso-Suarez**, IEEE Senior Member, is Associate Professor at the Physics Department, CENUR Litoral Norte, Universidad de la República, Uruguay, and Director of the Solar Energy Laboratory (<http://les.edu.uy/>). He has a B.S. and Ph.D. in Electrical Engineering and specializes in solar resource assessment and forecasting, particularly satellite-based solar irradiance modeling. He has co-authored more than 60 scientific articles on solar resource and solar energy applications.



**Germán Salazar** is a Professor of Environmental Physics at the National University of Salta (Argentina) and a Senior Researcher at the Non-Conventional Energy Research Institute (INENCO-CONICET) in Argentina. He has been conducting research on the characterization of solar radiation at high-altitude sites for the last 15 years.



**Fernando Nollas**, Researcher in solar radiation issues at the National Meteorological Service. He has a master's degree in renewable energy. He has experience in solar radiation data quality analysis as well as in the use of satellite databases and reanalysis.



**Olga Vilela** Coordinator of the Center for Renewable Energy of the Federal University of Pernambuco (CER-UFPE). She holds a PhD in Energy and Nuclear Technologies with a focus on solar energy. She is an associate professor at UFPE, conducting research in the areas of solar radiation forecasting and analysis; fault detection and diagnosis in photovoltaic plants; water pumping and desalination using solar power; solarimetry, and heliothermal systems.